

We are IntechOpen, the world's leading publisher of Open Access books Built by scientists, for scientists

6,900

Open access books available

186,000

International authors and editors

200M

Downloads

Our authors are among the

154

Countries delivered to

TOP 1%

most cited scientists

12.2%

Contributors from top 500 universities



WEB OF SCIENCE™

Selection of our books indexed in the Book Citation Index
in Web of Science™ Core Collection (BKCI)

Interested in publishing with us?
Contact book.department@intechopen.com

Numbers displayed above are based on latest data collected.
For more information visit www.intechopen.com



The Fukushima Disaster: A Cold Analysis

Cristian R. Ghezzi, Walter Cravero and
Nestor Sanchez Fornillo

Additional information is available at the end of the chapter

<http://dx.doi.org/10.5772/54262>

1. Introduction

The accident of Fukushima Daiichi Nuclear Power Plant on March 11, 2011, followed by an earthquake and tsunami at the Honshu island of Japan was one of the worst accidents in the history of mankind. It was classified as a level 7 nuclear accident, comparable to the Chernobyl accident in 1986. There was a general feeling of dissatisfaction about the information provided by the company Tokyo Electric Power Company (TEPCO), that operated the plant, and there were criticisms about the government decisions and on how the data about the measured dose rates in the island were interpreted. It is understood that in such a huge crisis, the people at charge in the company and in the government should not contribute to spread the panic, and it is useful to keep control of the situation. However, a flood of data invaded the news media and it turned difficult to harvest the truth among several contradictions, and to know about the destiny of a good portion of Japan and its population. Moreover, we scientist must feel compelled to clarify that truth, no matter if not directly working in the nuclear industry. We must feel an ethical and moral commitment to understand the situation in such a human calamity, because we are contributing directly or indirectly to the development of new technologies. It is necessary to learn from the errors of the past to plan carefully the highway towards the real progress. Our knowledge must be not abandon in hands of irresponsible people, but it must be driven to make our existence in this planet safer and happier.

This chapter is a technical report that exposes some basic concepts about nuclear physics, gives a concise chronology of the events at the Fukushima nuclear disaster, and analyzes a large database of dose measurements with a code specifically designed for it. It is not a document in favor or against the nuclear energy.

2. Chronicle of the disaster of Fukushima I

On March 11 of 2011, at 14:46 of Japan standard time, the earthquake Tōhoku impacted at the Honshu island of Japan. The earthquake had its epicenter approximately 70 kilometers east of the Oshika Peninsula of Tōhoku (coordinates 38°5'36" N 142°6'15"E) at the north of the main island of Japan, with a moment magnitude scale of 9 (equivalent to 8.9 in the Richter scale). For comparison, a ten kilotons nuclear explosion produces roughly a seismic wave of moment magnitude 4.8 [1]. The earthquake produced large accelerations on the ground of Fukushima I Dai-ichi nuclear power plant, at southwest of the epicenter (coordinates 37°25'17"N 141°1'57"E). The plant had six boiling water reactors, each one in separated containment buildings, and operated by the Tokyo Electric Power Company (TEPCO). The plant suffered accelerations in excess of 5 m/s², which is larger than the designed tolerances for the installations 2, 3 and 5, but within the tolerances of units 1 and 6 [2]. When the earthquake strikes, the reactors 4, 5, and 6 were in cold shutdown for maintenance, while reactors 1, 2, and 3 were in operation. However, reactors 1, 2, and 3 scrammed (shutdown automatically, see below) after the quake.

The plant lost its electric power, while the connection with the offsite power electric grid was lost due to the damages in the transmission lines by the earthquake. Thirteen electric diesel generators automatically came into operation to continue with the cooling of the six reactors. A giant tsunami wave followed approximately forty minutes after the earthquake, and surpassed the seawall of the plant of 5.7 meters, although the plant was about ten meters above the sea. The tsunami flooded the plant, and most of the diesel generators stopped working approximately one hour after the quake [3]. However, a diesel generator remained in operation and maintained the cooling capabilities of the cores and spent fuel pools of units 5 and 6 (units 5 and 6 are at 13 meters over the sea level).

After the diesel generators failure, an emergency power system sourced by electric batteries came into operation. But the batteries lasted eight hours, and although the replacement batteries arrived on time, it was impossible to connect the generators to the water pumps, since the connection point was flooded and was difficult to find the cables [4].

Therefore, TEPCO concentrated their efforts on establishing electric power from the offsite grid, and there was a long delay in connecting them to the cooling system.

2.1. Description of the reactors

A boiling water reactor (BWR) is a nuclear reactor that uses fresh water as moderator and coolant. The fuel rods are located in a pressurized container: the reactor pressure vessel (RPV). The control bars are inserted in from the bottom of the vessel, and together with the water are responsible for slowing down neutrons. The steam dryers are at the top of the RPV, and prepare the working fluid to enter the turbine. The RPV is itself contained in another container which is called drywell (DW). That container prevents that vapor vented from the reactor core enter into contact with the environment. In fact, the drywell contains (or is connected to) another vessel that surrounds the RPV bottom called the pressure sup-

pression chamber (SC) (also known as the wet well). During normal operation of the reactor there is a significant pressure difference between the RPV and the DW. If the RPV is vented to the DW, the condensate water is collected in the pressure suppression chamber. All this is in turn housed in a concrete structure, called the primary containment, which is intended to protect the indoor mechanically and to isolate the reactor.

The reactors are called based on core related systems, and that is done by a slash and a number after the acronym BWR: BWR/2 (/ 3, / 4 or / 5). It also makes the designation of the type of reactors the DW and SC that surrounds the RPV with the indicative Mark I or Mark II. The Mark I type has the DW electric bulb-shaped having the receiving SC -with toroidal shape- surrounding its base. The DW has an interconnecting vent network with the SC. The Mark II type has a DW in the form of a frustum of a cone or a truncated cone, surrounded around its base by a cylindrical SC separated from the DW by reinforced concrete slabs. At Fukushima Daiichi were located 6 units, the number 1 a BWR/3 Mark I. From 2 to 5 BWR/4 Mark I and number 6 was a BWR/5 Mark II^[1]. The units involved in the accident were BWR/3 and /4, all Mark I (see Table 1).

BWR/3 and BWR/4 have some similar features as the forced circulation systems with two recirculation loops and twenty single nosed-variable speed jet pumps. In both the “emergency core cooling system” (ECCS) high pressure pumping delivery point is in the vessel annulus via feedwater sparger, and for the same system the “low pressure core spray system” (CS) comprises two core spray (independent) loops. Also in both models the “hydrogen control short term” is provided by nitrogen inerting during normal operation.

Some pertinent differences between BWR/3 and BWR/4 are in the “reactor isolation pressure control”. Both have an “isolation condenser” (IC) and “safety relief valves” (SRV), but BWR/4 has steam condensing mode of the “residual heat removal system” (RHR). A remarkable difference is in the “reactor isolation inventory control”: BWR/3 has an isolation condenser while BWR/4 has a “reactor core isolation cooling system” (RCIC). While in the BWR/3 the shutdown cooling is performed by a “shutdown cooling system” or the residual heat removal system, in the BWR/4 only the last system is available. Something similar happens with the “containment spray and cooling”, BWR/3 has the option between “low pressure cooling injection” (LPCI) or RHR while BWR/4 only the last one. The high pressure pumping for the “emergency core cooling system” (ECCS) of the BWR/3 disposes of “feed-water pumps” or “high pressure cooling injection system” (HPCI). Only the last mentioned system is available in the BWR/4. A detailed description of the differences among reactors is shown in Table 6.0.1 of reference [6].

The accidents that occurred in all the reactors that were in operation followed an analogous path, as will be described in the following sections.

3. Main events after the earthquake

In the unit 1, the isolation condensers (IC) automatically actuated on the high reactor pressure after the scram, but were shutdown manually to prevent the cooling rate of the reactor

pressure vessel from exceeding a design limit (55 K/hour) [3,7]. The reason is because in the boiling water reactor the water acts as a neutron moderator for the nuclear reactions. Thus, a correct flow rate must be maintained to control the power of the reactor, because the flux of water allows fine reactivity adjustments. Depending on the quantity of vapor bubbles, the power of the reactor can vary. For example, if there are fewer bubbles, i.e., if the flux of water is greater, the neutrons are moderated to energies at which can be absorbed to produce fission. Thus, the power of the reactor increases when the flux of water is greater.

Unfortunately, when the tsunami struck, all the electric power was lost and the valves of the isolation condensers remained closed. Thus the IC of the unit 1 became useless. At units 2 and 3, the reactor core isolation cooling system (RCIC) started automatically after the earthquake and continued in operation for many hours after the tsunami. The unit 1 has an older reactor without a RCIC system.

	Unit 1	Unit 2	Unit 3	Unit 4	Unit 5	Unit 6
Reactor type	BWR-3	BWR-4	BWR-4	BWR-4	BWR-4	BWR-5
PCV type	Mark I	Mark II				
Max. pressure of RPV (MPa)	8.24	8.24	8.24	8.24	8.62	8.62
Max. press. of PCV (MPa)	0.43	0.38	0.38	0.38	0.38	0.28

Table 1.

Next it is given a short review of the events that lead to hydrogen explosions in three of the reactors within four days after the tsunami. The main events are condensed in the Appendix A.

3.1. Unit 1

All the valves of the isolated condenser were motor operated and were left in the closed position, as explained above, and this led to an increasing pressure inside the reactor 1 [7].

The pressure build up in the primary containment vessel was due to the liberation of steam - produced in the reactor pressure vessel- through the safety relief valves.

The measured pressure at the dry well was 0.84 MPa at 2:30 on March 12. This value doubles the pressure design for the dry well. It was argued that this pressure could not be due to steam alone, but built up from a mixture of steam and hydrogen [7].

The pressure in the reactor pressure vessel was as high as 6.9 MPa at 20:07 on March 11, but fell to 0.8 MPa at 2:45 on March 12. It is not clear if this depressurization occurred through the safety relief valves or if there was some cracking in the reactor pressure vessel within that interval [7]. If there were a meltdown of the fuel, and some portion fell to the bottom of the vessel, it is possible that it has damaged the reactor pressure vessel at the places where

the control rods are inserted. Thus, a leakage of the molten fuel to the primary containment vessel is possible [7]. This could be the cause of the depressurization at 2:45 on March 12. However, this is still a conjecture.

The injection of water to the reactor resumes at 5:46 on 12 March -using fire engines- 14 hours after the tsunami. But in this case, it is not clear if the pumps delivered the water at a pressure higher than the pressure in the reactor pressure vessel at that time (0.75 MPa). If the pressure of the pumps were lower, the water would have been supplied to the core about 22 hours after the tsunami, when the reactor pressure vessel was vented and depressurized [7].

As the fuel rods overheated, it was produced a water-Zirconium reaction that liberates hydrogen. The Zirconium of the zircaloy cladding of the fuel rods oxidizes with the steam according to the reaction:



The hydrogen is highly explosive and a deflagration or a detonation is easily triggered when mixed with air at a high pressure.

As the hydrogen had been vented to the secondary containment, an explosion occurs at 15:36 on 12 March 2011. The explosion blew the secondary containment without visibly damaging to the primary containment vessel. The sea water injection began at 19:04 on 12 March 2011.

3.2. Unit 2

The reactor core isolation cooling system (RCIC) operated continuously during three days and the water level on the reactor was maintained at its normal value. The RCIC stopped at 13:25 on March 14, 2011, by unknown causes. The pressure at the reactor pressure vessel began to rise, and the water level decreased.

The reactor was depressurized at 18:00 hs, through the safety relief valves. The seawater injection started at 19:54, and the water level recovery was confirmed at 22:00 on 14 March. An explosion occurs at 6:00 on 15 March. The suppression pool was assumed damaged, because of the large amount of contaminated water at the turbines building [7].

3.3. Unit 3

The reactor core isolation cooling operated normally for 20 hours after the tsunami, but failed at 11:36 on 12 March 2011. The operators started soon the high pressure core injection (HPCI), but it failed at 2:42 on 13 March 2011. It is yet not clear why the HPCI stopped. But a probable cause was the depletion of water in the condensate storage tank [7]. The reactor was left without water injection for more than six hours. The fresh water injection starts at 9:25 and changed to seawater injection at 13:12 on March 13, 2011. The pressure start to rise at the dry well and a series of venting operations followed to relief the pressure at the reac-

tor pressure vessel. The depressurization process led -like in the other reactors- to the accumulation of hydrogen at the secondary containment. So, an explosion blew up the secondary containment of unit 3 at 11:00 on March 14, 2011.

There is an interesting observation made by Gundersen [9] related with the hydrogen explosions in units 1 and 3. The explosion in unit 1 occurred mainly sidewise, while explosion in unit 3 occurred visibly in the vertical direction and apparently the explosion was much more violent. Gundersen claims that explosion in unit 3 was a hydrogen detonation, while explosion in unit 1 was a hydrogen deflagration. A detonation is a supersonic combustion wave (respect to fuel), while a deflagration is a subsonic combustion. Gundersen noticed that this could be an indication of prompt criticality in the spent fuel pool of reactor 3 [9]. Although this is a possible explanation for the difference in the explosions, it must be noticed that there are other factors that could alter the development of the explosion, i.e., the preheating of the gas before the ignition of the combustion can lead to a detonation. The development of a detonation depends on the temperature gradients of the gas. Thus, the combustion mode depends on the complex history in which the hydrogen was released to the second containment vessel. If the hydrogen was promptly released the gradient could be too steeply to develop a detonation. On the other hand, turbulence in the fuel mixture can also lead to a deflagration to detonation transition, since the turbulence can induce a shallow temperature profile, mixing hot fuel regions with cold ones.

4. Basic concepts

Radioactivity is the spontaneous disintegration of an atomic nucleus. In the radioactive decay the nucleus decay in lighter nuclei, which are the fragments of the nuclear disintegration, in addition there could be an emission of neutrons, gamma rays, electrons and neutrinos.

Several radioactive isotopes are man-made, but there are also radioactive traces found in some minerals, in soils; in the plants; in the animal's tissue; in the air; and in the water.

Uranium -as other heavy elements- is radioactive and its main isotope decays according with the reaction:



That is the uranium-238 decay into thorium-234, emitting an alpha particle α (${}^4_2\text{He}$). The daughter isotope thorium is also radioactive and decays as:



Where the first element on the right side is protactinium, the second particle is an electron (also called β^- beta particle), and the last particle is a neutrino.

These two reactions are the start for a long chain of reactions that ends at the stable isotope of lead $^{206}_{82}\text{Pb}$. There are similar chains for uranium-235 and thorium-232.

Element	Mean life
caesium-137	30.3 years
radon-222	3.82 days
iodine-129	1.7×10^7 years
iodine-131	8.04 days
strontium-90	29.1 years
uranium-235	7.04×10^8 years
uranium-238	4.46×10^9 years
plutonio-239	2.41×10^4 years

Table 2.

The mean life of a radioactive nucleus t_h (half-life) is the time in which half of the radioactive sample decays. The radioactive decay is essentially probabilistic, and its law is a negative exponential of time:

$$N(t) = N_0 e^{-t/t_m}, \quad (4)$$

where t_m is the mean-lifetime. The meaning of this law is that the number of parent nucleus in a sample at a given time, $N(t)$, diminishes exponentially with time from the initial number N_0 . Some mean lifetimes for known radioactive nucleus produced in a nuclear reactor are given in Table 2. The activity (A) of a radionuclide is the number of decays per unit time:

$$A = N / t_m. \quad (5)$$

Thus, the larger is the radionuclide sample, the higher will be its activity. For the same amount of nuclide the activity is higher for the radionuclide with lower mean lifetime. The activity is measured in becquerel (Bq), honoring the scientist who discovered radioactivity. A Bq is equivalent to one disintegration per second. The other commonly used unit is the curie (Ci), equal to 3.7×10^{10} disintegrations/second, which is equivalent to the activity of one gram of radio.

The fission of the uranium-235 occurs by means of the absorption of thermal neutrons produced in other radioactive decays. The most probable reaction gives krypton and barium:



The total energy release on the induced fission of ${}^{235}_{92}\text{U}$ is on average 205 MeV [10]. From this total the neutrinos escape unimpeded with 12 MeV, while the remaining energy is distributed in the kinetic energy of the fission fragments, the neutrons, the photons, the betas, plus the delayed gammas and betas. Thus, the fission of uranium produce a useful energy of 190 MeV, which is equivalent to 3.04×10^{-11} J. The number of fissions to produce a watt-second is:

$$1 / (3.04 \times 10^{-11}) = 3.3 \times 10^{10} \text{ decays},$$

which is roughly the number of decays in one gram of radio during one second. Thus, in order to produce a megawatt of thermal energy per day is required, roughly:

$$10^6 \text{ W} (3.3 \times 10^{10} \text{ decays} / \text{W} \cdot \text{s}) 86400 \text{ s} / \text{day} = 3.3 \times 10^{21} \text{ decays} / \text{day}.$$

But, a mol of uranium-235 has the Avogadro number of atoms (6×10^{23}). So, the consumption of uranium per megawatt is:

$$3.3 \times 10^{21} (\text{decays} / \text{day}) 235 \text{ grams} / (6 \times 10^{23}) = 1.3 \text{ grams} / \text{day},$$

without considering the efficiency of the chain reactions. This is equivalent to 1.3 kg/day of uranium-235 for a 1000 MW power plant, or 474 kg of uranium-235 per year (or equivalent 27 kW/kg, taking into account an enrichment of 1%). If reactor 1 of Fukushima has 78 ton of fuel in its core, and assuming the fuel is new and enriched at 1.5 %, there is enough fuel for 2.5 years. The quantity of spent nuclear fuel in the pool of each reactor is [11]:

- Reactor No. 1: 50 ton of nuclear fuel
- Reactor No. 2: 81 ton
- Reactor No. 3: 88 ton
- Reactor No. 4: 135 ton
- Reactor No. 5: 142 ton
- Reactor No. 6: 151 ton

Each reactor at Fukushima has less than 100 ton of nuclear fuel.

4.1. Why the fossil fuel is less viable and produces a large damage to the environment?

It can be shown that is required millions of times more mass of carbon than uranium to produce the same amount of energy. The carbon gives 32 kilojoules per gram of energy. In order to produce 1000 MW of energy it is required [12]:

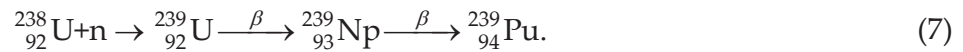
$$(1000 \times 10^6 \text{ joules} / \text{s} \times 86400 \text{ s} / \text{day}) / (32000 \text{ joules} / \text{gr}) = 2.7 \text{ millions of ton} / \text{day}.$$

Thus, the fossil fuel is highly contaminant to our atmosphere. However, on the view of the Chernobyl and Fukushima nuclear accidents, we must know reconsider which energy source is more dangerous for human life.

4.2. Induced fission

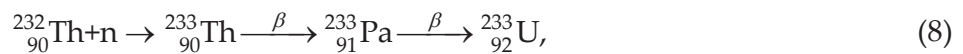
The objective of a nuclear reactor is to produce a self-maintained and controlled chain reaction of a fissionable element.

There are two classes of fissionable materials, depending on how they behave when absorbing a neutron [13]. A fissile material is one that will undergo a nuclear fission when bombarded by neutrons of any energy. A fertile material is one which after capturing a neutron, will transmute by radioactive decay into a fissile material. The uranium-235 is the only fissile material found in nature. The fertile material ^{238}U becomes radioactive and decays in series of beta decays into ^{239}Pu after capturing a neutron:



The plutonium-239 is a fissionable material, i.e., it will decay if a neutron strikes it. The ^{239}Pu has a very large half-life, so it can be stored and used as a reactor fuel (see the table 1).

The thorium-232 is another fertile material found in nature. It decays in a series of beta decays after absorbing a neutron according to the reaction:



where the uranium-233 is a fissile material.

In general, when a neutron impinges on the nucleus of uranium-235, it breaks into fragments and there are a mean of 2.4 neutrons emitted, gamma rays, and neutrinos:



The uranium-235 fission leads to a neutron multiplication; each neutron emitted in the fission has the potential to lead to a new fission in the fuel sample. The reactions will continue until all the uranium-235 decay, or until no free neutrons are left in the sample, i.e., until all the neutrons escape from the boundaries of the fuel or are absorbed by another non-fissionable material.

A typical fission reaction for uranium-235 is:



The fission fragments in this reaction are also unstable because their neutron to proton ratio is too large. The fission fragments decay mostly by beta particle emission accompanied by gamma rays. The decay occurs in several stages until reaching the stable nuclei branch, for example:



the reaction for strontium is:



The energy release from the nuclear fission is distributed into the kinetic energy of the fission fragments, beta particles and neutrons, and in the energy of the gamma rays and neutrinos.

	MeV
Fission fragment kinetic energy	166
Neutrons	5
Prompt gamma rays	7
Fission products gamma rays	7
Beta particles	5
Neutrinos	10
Total	200

Table 3.

The energy balance for the decay of a uranium nucleus is given in the Table 3 [10, 12].

A chain reaction is self-maintained when the fuel do not need to be bombarded by external particles to maintain the fission process [12].

The chain reaction will be self-sustained and maintained in time if the mass of the nuclear fuel is larger than a critical mass value. The critical mass is the quantity of matter necessary to compensate the neutrons loss across the boundaries of the fuel, in such a geometric configuration that allows the chain reactions.

Fissile materials can be produced in the core of a reactor if fertile material is mixed with the nuclear fuel. In the decay of ${}^{235}\text{U}$ there are enough neutrons to sustain a chain reaction and to convert fertile to fissile material. If a nuclear reactor produces more fissile material than it consumes, it is said that the reactor is a breeder. As most reactors use natural uranium, or

uranium with low enrichment, there are enough ^{238}U -a fertile material- in the fuel to be converted into plutonium [10,13].

However, the design of a breeder is not easy due to the absorption of neutrons by other materials. Moreover the neutrons can leak through the boundaries of the fuel. Thus, most reactors are not breeders [13].

4.3. Neutron cross-section for fission

The cross section of ^{235}U and ^{238}U , as a function of the energy of the incident neutrons is of great relevance to sustain a chain reaction.

Since neutrons are uncharged they do not find a coulomb barrier to reach the nucleus; thus the neutrons can interact with the nuclei even if they have very low energy [10,12]. At low neutron energies the exothermic nuclear reaction rate is roughly independent of the energy and proportional to the density of the incident flux of neutrons [10]. The reaction rate for nuclear fission induced by neutrons can be written as [10,12]:

$$R = \rho_n v \sigma \quad (13)$$

where R is the reaction rate; ρ_n is the neutron density; v is the mean speed of the neutrons and σ is the cross section of the target nucleus. Thus, the cross section at low energies is proportional to the inverse of the speed of the neutrons, or equivalently, inversely proportional to the square root of their energy:

$$\sigma \propto \text{const} / v. \quad (14)$$

This law was experimentally observed [10,12,13]. The dependence of the total cross section with energy changes very fast for neutron energies close to the resonances of the compound nucleus. In this case, the cross section is characterized by a series of narrow resonance peaks, and is expressed by the Breit-Wigner formula [10]. These peaks are due to the excited states of the compound nucleus (see fig 9.1 in ref [10]).

The principal elements in the fuel of a reactor are uranium-235 and uranium-238, which are found in the nature in the proportions 0.72 % and 99.27 % respectively [12].

The neutron absorption cross section can be divided into two parts, the fission cross section and the radiative cross section. In the radiative capture, a compound nucleus is formed with gamma ray emission (for example ^{236}U). In addition some of the neutrons can suffer inelastic or elastic scattering from the nucleus without being absorbed.

The total cross section for ^{235}U at energies below 0.1 eV is mostly due to the fission cross section (84 %), while the remaining are due to radiative capture (16 %). In this energy range, the total cross section follows the $1/v$ law. In the range between 1 eV and 1 keV is the resonance region. In this region the cross section varies very rapidly with the energy. In the third re-

gion for energies larger than 1 keV, the cross section for ^{235}U is predominantly due to scattering (inelastic at energies larger than 14 keV). The fission cross section is lower than the total cross section, and much lower than in the first energy range [10].

The cross section for ^{238}U is almost constant in the low energy region, and is predominantly due to elastic scattering and radiative absorption. The fission cross section starts to be significant above 1.4 MeV, although it remains a small fraction of the total cross section.

4.4. Chain reaction

As described above the neutron cross section for ^{235}U fission, is much higher for low energy neutrons. The fission process produces fast neutrons with energies in the interval $0.1 \text{ MeV} < E < 10 \text{ MeV}$, and are predominantly emitted with 0.75 MeV. Thus, the neutrons must be slowed down in the reactor to energies at which they can be captured in the ^{235}U with greater probability. The neutrons transfer their energy to the nuclei by multiple scattering, until reaching an approximately thermal distribution, in which they can be captured by the fissionable fuel [13]. The so called thermal neutrons have a range of energies in the interval $0.001 \text{ eV} < E < 1 \text{ eV}$.

The mean free path of a neutron of 2 MeV in the fuel is around 3 cm [10]. However, the probability of inducing a fission in one collision is rather low at that energy (18 %). The probability will increase significantly after six collisions (number of collisions \times probability of fission ~ 1). If the neutron follows a random walk through the fuel, it will move about $\sqrt{6} \times 3 \text{ cm} \approx 7 \text{ cm}$ from the starting point before inducing fission [10]. If the probability that a neutron induce a new fission is q , then on average each neutron will create $(\nu q - 1)$ additional neutrons, where ν is the mean number of neutrons emitted per fission.

If there are $n(t)$ neutrons at time t , then at time $t + \delta t$ there will be an additional number of neutrons proportional to the number of neutrons $n(t)$, times the number of neutrons produced by each of these, times the fraction of time they had to react $\delta t / t_p$, where t_p is the time required to produce a fission at the indicated energy, so [10]:

$$n(t + \delta t) = n(t) + (\nu q - 1)n(t)\delta t / t_p. \quad (15)$$

This equation gives the differential equation for neutron multiplication:

$$\frac{dn(t)}{dt} = (\nu q - 1)n(t) / t_p, \quad (16)$$

that has the solution [10]:

$$n(t) = n_0 e^{(\nu q - 1)t / t_p}. \quad (17)$$

Thus the number of neutrons can grow exponentially if $\nu q > 1$ (supercritical assembly), or decrease exponentially if $\nu q < 1$ (subcritical assembly). The probability q depends on the geometry and size of the sample, and on the energy of the neutrons. The characteristic time for fission is $t_p=10^{-8}$ s, this means that for a supercritical assembly there will be a huge amount of energy liberated in less than a microsecond. The critical radius for a sphere of ^{235}U is about 8.7 cm, and the critical mass is 52 kgs [10].

The reactors have control rods containing boron, or cadmium, which can absorb neutrons in the thermal range. So, inserting or withdrawing the control rods in the reactor core can modify the reactor power. The reactor must be operated at criticality, but is important that criticality is achieved taking into account the delayed neutrons, and not the prompt neutrons alone. This is because, the prompt neutrons have lifetimes of the order of 10^{-3} s, and this is a very short time to mechanically control the power output of the reactors. The delayed neutrons led to a better timescale to control the reactor. Moreover, the reactors must be designed for thermal stability, i.e., the probability for a new fission is such that [10]:

$$\frac{dq}{dT} < 0, \quad (18)$$

thus an increase in the temperature of the reactor diminishes the reactivity.

4.5. Nuclear fuel of the reactors

Natural uranium has more than 99 % of ^{238}U , and less than 1 % of ^{235}U . When a neutron is emitted in the fission process at 2 MeV, it will more probably interact with the ^{238}U , through inelastic scattering, leaving it in an excited state. After a few scatterings the neutron will lose its energy capable to induce fission in ^{238}U . So, the neutron must find a ^{235}U to induce fission, but as it is so much less abundant it is more probable the neutron is captured in a ^{238}U resonance to form ^{239}U with the emission of a gamma ray. Thus, the proportion of fission neutrons that induce further fission in natural uranium is rather low, and a chain reaction can not be sustained [10].

However, a technology has been developed to produce a chain reaction from natural uranium. The Fukushima Daiichi reactors are thermal reactors. In a thermal reactor the fuel is the ceramic uranium dioxide, and is contained in an array of thin rods containing the fuel pellets. In the reactor the fuel is surrounded by a large volume filled with a material of low mass number, called the moderator. The neutrons can lose their energy in the moderator before encountering a uranium nucleus. Thus the neutron cross section for ^{235}U fission increase and is much larger than for ^{238}U , compensating the low concentration of uranium-235. The neutrons are called thermal because their energy corresponds to the operation temperature of the reactor ($0.1 \text{ eV}=1160 \text{ }^\circ\text{K}$).

The capture of neutrons at thermal energies, lead to the fission of the ^{235}U with large probability, and thus, the chain reaction is made possible with natural uranium using this technology.

The moderator can be ^{12}C , or heavy water (D_2O). But, if the reactors use enriched uranium, the reactor can be moderated using ordinary water.

The reactors at Fukushima have low enriched uranium fuel (LEU), except the unit 3 that has a low percentage (~6 %) of MOX (mixed oxide) consisting in a blend of uranium oxide (UO_2) and plutonium oxide (PuO_2) [15]. The mixture has 7 % plutonium and the rest is natural uranium. The LEU is enriched to ~3 % of uranium-235.

4.6. The reactor power

The thermal power generated by a nuclear reactor is approximated by the formula [12]:

$$P = \varphi N V \sigma_f w, \quad (19)$$

where $\varphi = n v$, is the neutron flux; N is the number of fissile nuclei ^{235}U per unit volume; V is the total fuel volume; σ_f is the neutron cross section for fission; and w is the mean energy liberated per fission.

The efficiency of a nuclear reactor is 1/3 the total thermal power. There is a distinction in the notation between units of megawatt of thermal power -which is the total generated power- indicated as MWt, and the total generated electric power -the energy converted to work- indicated as MWe.

The reactors of Fukushima generated the following energy [18]: i) the unit 1 has a General Electric reactor of 460 MWe; ii) unit 2, has a General Electric reactor of 784 MWe ; iii) unit 3 has a Toshiba reactor of 784 MWe; iv) unit 4, has a Hitachi reactor of 784 MWe; v) unit 5 has a Toshiba reactor of 784 MWe; vi) unit 6 has a General Electric reactor of 1100 MWe.

4.7. Power of the reactor after shutdown

After the scram of the reactors the control rods were inserted into the core, and the uranium-235 fission stopped. However, the fuel rods containing the fission products which are neutron rich, decay emitting beta rays and gamma rays as well. So, the fuel rods continued producing heat after the scram.

The empirical expression for the power of heat decay P is given by the formula [10, 12]:

$$P = 0.07 P_0 [(\tau - \tau_s)^{-0.2} - \tau^{-0.2}], \quad (20)$$

where P_0 is the nominal reactor power, τ is the time since the reactor startup in seconds, and τ_s is the time of reactor shutdown since the startup. This expression has an acceptable error in a certain time interval ranging from 10 seconds and 100 days.

The nominal power for reactor 2 and 3 is 2352 MWt. If the rods have a life of one year, the decay power after one day is: 11.7 MW; after one week is: 6.3 MW; after one month

is: 3.5 MW; and after one year is: 0.7 MW. If the lifetime of the rods is larger the decay power will be higher.

5. The importance of blogging in crisis times

The Ministry of Education, Culture, Sports, Science and Technology (MEXT) of Japan published real time radiation measurement data acquired by the “System for Prediction of Environment Emergency Dose Information” (SPEEDI). However, this data was not very accessible for processing, as was published in html format and in Japanese. Mr. Marian Steinbach, started a “Google Docs Spreadsheet” and called for help to the online world to collect the data [21]. The results are compressed in one file (station_data_1h.csv.gz) that contains the following information:

- a. Station identifier: a number identifies each station that performs a measurement.
- b. Time UTC (in order to convert to JST just add nine hours).
- c. Radiation dose measured by the stations. The measurements are in nGy/h, or equivalently in nSv/h (with a quality factor of one).
- d. Rain precipitation in mm.

For example, the file looks like these three sample lines:

```
1150000004 - 28/02/2011 15:00 - 370
```

```
1020000026 - 28/02/2011 15:00 - 21 - 0
```

```
1020000004 - 28/02/2011 15:00 - 20 - 0
```

The measurements are made every ten minutes in more than two hundred stations along Japan, and the file starts in March 1, 2011, until the present. So, the archive has more than 600 Mbytes today, and it requires near 2 Gbytes of free RAM memory to read it with conventional text processors. It’s good to emphasize here the great effort made by several bloggers to collect all the measured data (see for example Refs. [20, 21, 22]). The data must be combined with another archive providing information on each station: site name, site identifier, location, city, prefecture, and geographic coordinates (see [24]). The authors of the present chapter programmed a Fortran code to retrieve information from this data base.

Some data on the spreadsheet indicates measured values equal to -999, it is presumed that it is due to a saturation of the detectors that can measure dose rates up to 1000 mSv/h. In addition, several stations close to the nuclear power plant stopped measuring dose rates on March 11, and restarted on September 21, 2011 [21].

The action of bloggers helped to understand the critical situation at Fukushima and bring calm to the general population. It was an alternative and reliable source to retrieve information about the crisis and (in several cases) the information provided was not so confusing like in the main news channels.

6. Study of the radiation distribution

In a simplified model of the radiation emitted from the nuclear power plant, it could be assumed that the particles will travel radially out from a point source, emitting S particles per second isotropically. The particles can survive a certain distance without scattering with other particles, depending on the macroscopic cross section for scattering and the density of target nuclei. If there is a certain amount of radioactive particles being emitted from the site accident, the flux of particles will be attenuated by a geometric factor with the distance and by the scattering with the atoms of the atmosphere.

The flux of particles passing through a sphere of radius r is:

$$\phi(r) = \frac{e^{-\Xi r}}{4\pi r^2} S, \quad (21)$$

where Ξ is the macroscopic cross section (the macroscopic cross section depends on the microscopic cross section σ and the number of air nuclei per unit volume: $\Xi = N \sigma$). Thus, it is expected that if the Fukushima nuclear reactors are emitting radioactive particles to the air isotropically, the measured radiation must fall faster than r^{-2} with distance. Of course, the hypothesis of isotropic emission of particles is not true in the case of Fukushima, since there was an important wind carrying the radioactive emission to the sea in the days following the accident. This was a good factor within the disgrace of the accident, since the wind dragged the radiation out from populated zones.

It is difficult to make correct predictions on the nuclear fallout without a detailed numeric simulation taking into account the full meteorological data: including wind direction, wind speed, and rain fall at each date.

The database of dose measurements was surveyed to provide a description of the dependence of the radiation versus time, and radiation versus distance from Fukushima Daiichi nuclear power plant.

Since there are two widely used systems of units to measure the radiation dose, we clarify the definitions and the conversion between the two systems of units.

A dose is the quantity of energy absorbed by a kilogram of exposed tissue to the radiation. In the International System, a dose unit is the gray (Gy) equivalent to 1 joule/kg. The other commonly used unit is the *rad*, equivalent to 100 erg/gram, or equivalent to 0.01 Gy.

As the damage produced on the tissue depends on the radiation type, i.e., alpha particles; neutrons; beta particles; or gamma rays, it is used the concept of quality factor QF , and it is defined a *dose equivalent* as [12, 25]:

$$H = (QF) \times D. \quad (22)$$

mSv/h	$\mu\text{Sv/h}$	nSv/h	mrem/h
0.0001	0.1	100	10^{-6}
0.001	1	1000	0.00001
0.01	10	10000	0.0001
0.1	100	100000	0.001
1	1000	10^6	0.01
10	10000	10^7	0.1

Table 4.

A larger equivalent dose produces a larger damage to the human health.

If D is given in Gy, the units of H are sieverts, while if D is measured in rad, H are in rem.

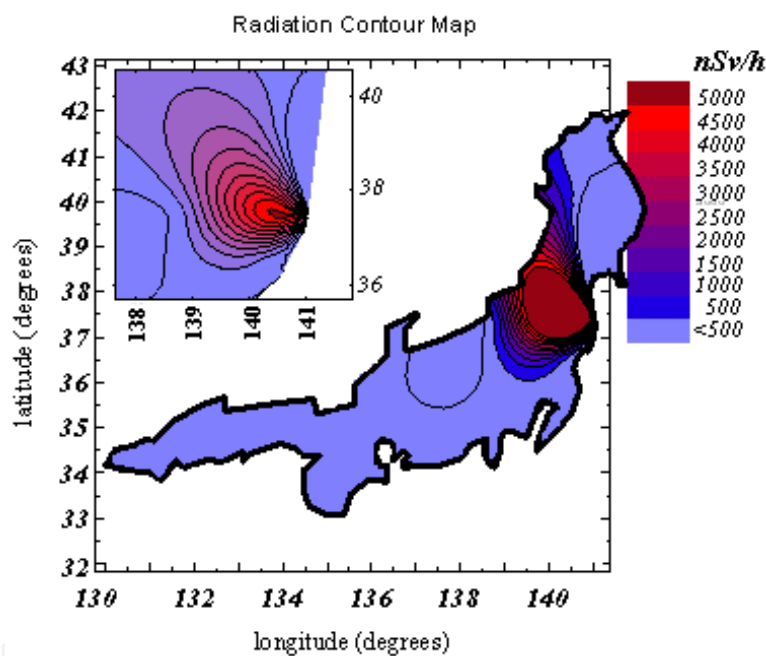


Figure 1. Radiation contour map as November 15, 2011

For fast interpretation and comparison of the results with the data found in the literature, the Table 4 gives the conversion between commonly used units and its multiples for the measured dose equivalent rate, spanning all the relevant range of values for the Fukushima accident. In the analysis of the data is implicitly assumed that the quality factor is one, as is commonly assumed in the literature about Fukushima, i.e., the measurements are expressed as mGy/h or mSv/h, indistinctly, although this is not strictly correct, since the damage depends on the type of radiation and the form of exposure.

The occupational annual dose to individual adults, except for planned special exposures, is a total effective dose equivalent equal to 50 mSv [25]. For the individuals the radiation dose equivalent limit is 5 mSv [25]. This means that in normal conditions a person must not re-

ceive a dose equivalent larger than $0.6 \mu\text{Sv/h}$. In the next set of figures we show the results of the database analysis. The Figure 1 shows the radiation contour map for the Honshu island of Japan, as November 15, 2011, at 15:20 UTC. The silhouette of the island is representative. The color scale increase in units of 500 nSv/h . The darkest red shows the region in which the radiation is above 5000 nSv/h . Note that the background radiation, according to the database, is roughly 30 nSv/h . The limit for non-nuclear workers is in the range $570 \text{ nSv/h} / 2283 \text{ nSv/h}$ ($5 \text{ mSv}/20 \text{ mSv}$ annual).

The inset shows the same map but with contour lines in intervals of 1000 nSv/h . The darkest red –in the inset- shows the region in which the radiation is above 10000 nSv/h .

Caveat: the radiation contour map displayed could be scary, but as it will be shown the radiation falls with time due to the half life of the radioactive isotopes and by the action of the wind. There is an important contribution from atmospheric radiation to this map, and not necessarily all the radiation was deposited in the ground. Moreover, this is a contour map and do not mean that a high radiation level was actually measured in all the shadowed areas, but on some point located within it at the date indicated. The map is more representative of the spatial distribution of the radiation at the indicated date.

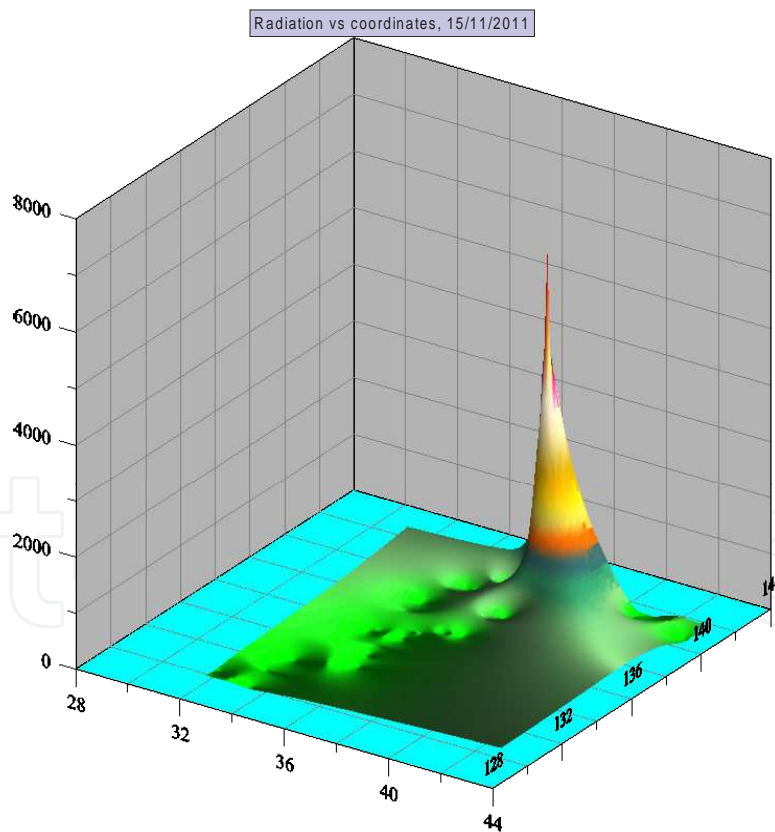


Figure 2. Spatial distribution of the radiation as function of the geographic coordinates.

The release of radioactive isotopes was due to the necessary venting of the reactor pressure vessel and of the dry well of the reactor. The venting was done to reduce the pressure inside

the reactor. The release of radioactive particles was worsened with the explosion of the secondary containment that occurred due to the hydrogen explosions of units 1 and 3, and a breach in the suppression chamber of unit 2 (see the Appendix).

The incident was rated at level 7 according to the International Nuclear Event Scale. However, the total amount of iodine-131 was 73 % of those measured at the 1986 Chernobyl nuclear disaster, and the amount of caesium-137 released from Fukushima is around 60 % of the amount released from Chernobyl [27].

The main isotopes released at Fukushima have been iodine; caesium; strontium; and plutonium. These radioactive elements have been released to the atmosphere and to the Pacific Ocean.

Prefecture	City/Station	Distance (km)	Rad (nGy/h)
Fukushima	Futaba Town – Yamada	0,7	27210
Fukushima	Ono Ookuma	2,5	6417
Fukushima	Futaba Town – Shinzan	3,1	5588
Fukushima	Futaba Town - Kooriyama	4,3	1698
Fukushima	Namie Town - Namie	7,1	1167
Fukushima	Yonomori Tomioka Town	7,3	4461
Fukushima	Namie Town – Kyohashi	8,1	528
Fukushima	Tomioka Tomioka Town	10,1	3612
Fukushima	Kamikooryama Tomioka Town	10,8	1787
Fukushima	Tomiokacho	11,8	2157
Fukushima	Matsudate Naraha town	13,6	1434
Fukushima	Shigeoka Naraha Town	14,5	1177
Fukushima	Yamadaoka Naraha Town	19,1	352
Fukushima	Futatsunuma Hirono town	22	611

Table 5.

The Figure 2 shows the radiation landscape on November 15, 2011, at 15:20 UTC. The radiation dose rate in nGy/h is a function of the geographic coordinates, i.e., latitude and longitude, in degrees. At this date, the radiation peaked 27210 nGy/h at the nuclear station, which is 50 times more radiation than the maximum limit for non-nuclear workers. The second peak was at Ono Ookuma (distance 2.5 kms), measuring 6417 nGy/h. There was another peak of 5588 nGy/h at Futaba Town, Shinzan (3.1 kms). For clarity, the Table 5 shows the measurements above 100 nGy/h, for the same date as above, specifying the location of each station and its distance to the power plant.

Prefecture	City/Station	Distance (km)	Rad (nGy/h)
Ibaraki	Onuma Hitachi City	104	446
Ibaraki	Mayumi Hitatoota City	106,7	324
Ibaraki	Kuji Hitachi City	107,8	775
Ibaraki	Kume Hitatoota City	108,4	147
Ibaraki	Isobe Hitatoota City	108,5	487
Ibaraki	Ishigami Tokai	110,5	724
Ibaraki	Toyooka Tokai Village	110,5	387
Ibaraki	Nemoto Hitachioomiya City	111	266
Ibaraki	City Nukata Naka	111,7	319
Ibaraki	Funaishikawa Tokai	113	192
Ibaraki	Kadobe Naka City	113,1	735
Ibaraki	City Uridura Naka	113,4	188
Ibaraki	Muramatsu Tokai-mura	113,8	251
Ibaraki	City Yokobori Naka	114,3	309
Ibaraki	Oshinobe Tokai Village	114,5	306
Ibaraki	City Kounosu Naka	115,8	401
Ibaraki	Sawa Hitachinaka City	116,7	734
Ibaraki	Sugaya Naka City	117,1	234
Ibaraki	Mawatari Hitachinaka City	118,5	311
Ibaraki	Hitachinaka Hitachinaka City	119,5	351
Ibaraki	Godai Naka City	120	398
Ibaraki	Ajigaura Hitachinaka City	120,1	199
Ibaraki	Horiguchi, Hitachinaka City	122,7	1045
Ibaraki	Sawa Yanagi Hitachinaka City	124,2	238
Ibaraki	Ishikawa, Mito	125	216
Ibaraki	Isohama Oarai Town	128,3	162

Table 6.

According to these measurements, the region beyond 20 km has an “acceptable” level of radiation at the indicated date, although it is still twice greater than the background up to distances of 140 km (not shown in the table).

The following figures show the decrease of the radiation with the radial distance from the nuclear power plant. The vertical axis displays the radiation dose in nGy/h, in logarithmic scale, while the horizontal axis displays the radial distance to the nuclear power plant in km. The Figure 3 shows the radiation versus distance as March 15, 2011, at 15:20 UTC time. In this date, there are no stations collecting data closer than 100 km from the nuclear plant. There was a blackout of several stations that recovered after September 21, 2011, thus the data is incomplete. There is a large scatter of the data, which may be due to the topography of Japan, the action of the wind, and the rain fall in each location.

15/03/2011, 15:20 hs

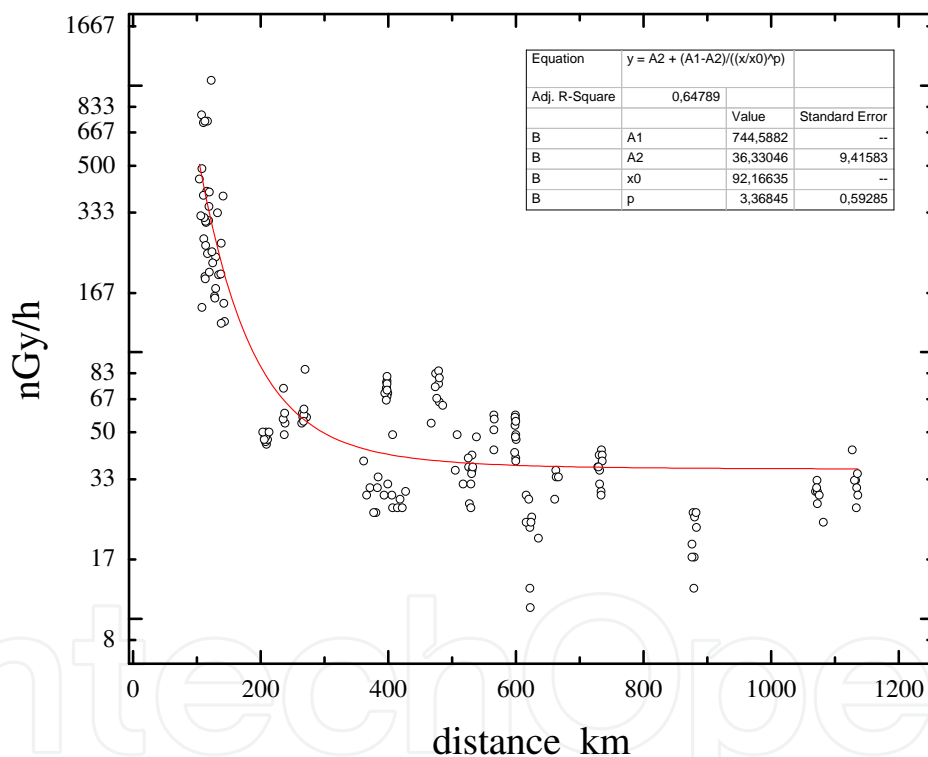


Figure 3. Radiation versus distance as March 15, 2011.

A non-linear fit of the data was performed with Origin 8.0. The result of the fit is shown as the red curve in the figures. It was found that the optimal fit is obtained with a function proportional to $1/r^p$, with $p=3.36$. Thus, the radiation decrease faster than $1/r^2$, as expected.

As shown in the figures and tables the radiation has a large heterogeneous distribution, sometimes with large variations in dose measurements (>200 nGy/h) in very short distances (sometimes of the order one hundred meters).

Prefecture	City/Station	Distance (km)	Rad (nGy/h)
Ibaraki	Onuma Hitachi City	104,1	166
Ibaraki	Kuji Hitachi City	107,8	180
Ibaraki	Toyooka Tokai Village	110,5	120
Ibaraki	Ishigami Tokai	110,5	122
Ibaraki	Muramatsu Tokai-mura	113,8	113
Ibaraki	Sawa Hitachinaka City	116,7	112
Ibaraki	Mawatari Hitachinaka City	118,5	129
Ibaraki	Hitachinaka Hitachinaka City	119,5	177
Ibaraki	Ajigaura Hitachinaka City	120,1	116
Ibaraki	Horiguchi, Hitachinaka City	122,7	136
Ibaraki	Isohama Oarai Town	128,3	117
Ibaraki	Town Oarai Onuki	129,9	125
Ibaraki	Hiroura town Ibaraki	132,6	147
Ibaraki	Tasaki Hokota City	136,4	107
Ibaraki	Ebisawa town Ibaraki	137,7	110
Ibaraki	Araji Hokota City	138,3	128
Ibaraki	Tsukuriya Hokota City	138,4	158
Ibaraki	Momiyama Hokota City	141,5	189

Table 7.

As March 15, 2011, due to the stations blackout in Fukushima the largest radiation measurements made were in the Ibaraki prefecture as shown in the Table 6.

The Table 6 displays the radiation measurements larger than 100 nGy/h. It is possible to appreciate the large dispersion in the measured radiation with the distance. For example, there is a large difference in the dose measured at Funaishikawa Tokai with what is measured at its neighbor Kadobe Naka city.

The Figure 4 displays the radiation versus the radial distance at July 15, 2011, at 15:20 UTC time. It is seen that the non-linear fit decrease slower with the distance. The best fit gives $p=1.5$, so in this case, the rate of decrease is less than the r^{-2} law. This could be to the action of the wind, not taken into account in the Equation (21). Moreover, the radioactive particulate could act as nucleation centers to form rain drops, and the rain could significantly modify the radiation distribution.

In addition, is observed that the radiation distribution at this date is more scattered.

It is seen that the maximum radiation dose rate at Ibaraki decreased respect to the measurements made in March. The maximum dose rate was 189 nGy/h at Momiyama Hokota City (141.5 km from Fukushima Daiichi I, see Table 7).

The Figure 5 shows the radiation decrease with distance as November 15, 2011. The non-linear fit gives $p=1.09$, thus, the radiation profile is becoming flatter as time goes by. The stations were recovered near Fukushima, so the readings are higher.

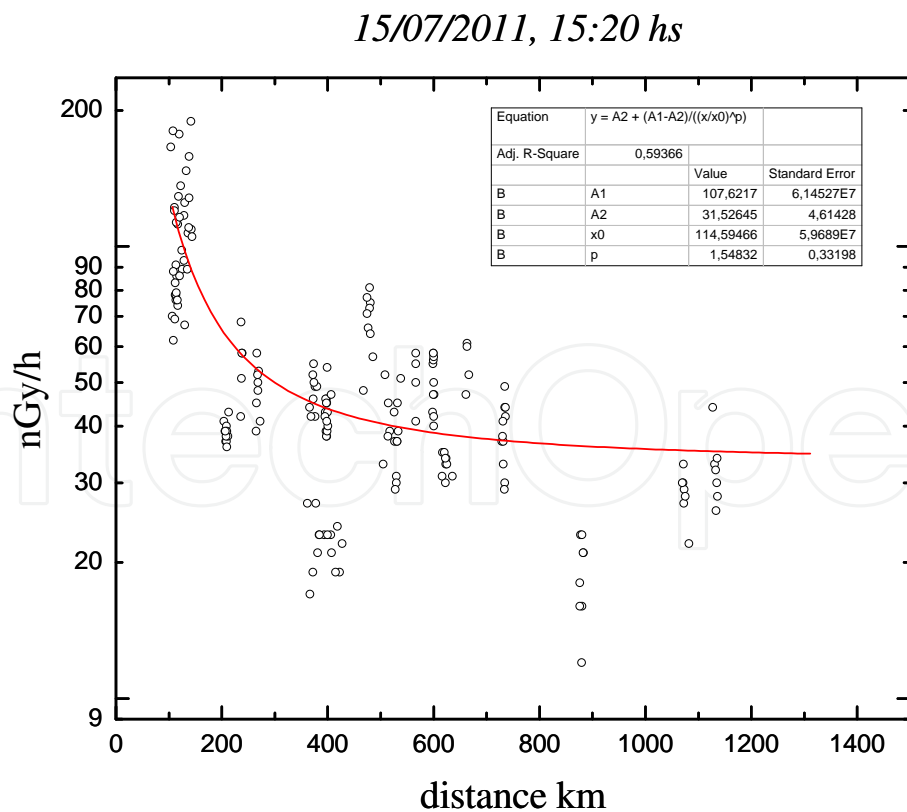


Figure 4. Radiation versus the radial distance at July 15, 2011

There are records of dose rates as high as 27210 nGy/h, near the central (see Table 5).

The following figures show the decrease of radiation with time at two locations. The Figure 6 shows the decrease of radiation with time at the nuclear power station. It is seen that the time evolution can be approximated with a straight line in the indicated period of time. The slope of the line is roughly 31 nGy/day. A decreasing exponential with a half life of 3.4 years can also be adjusted (not shown).

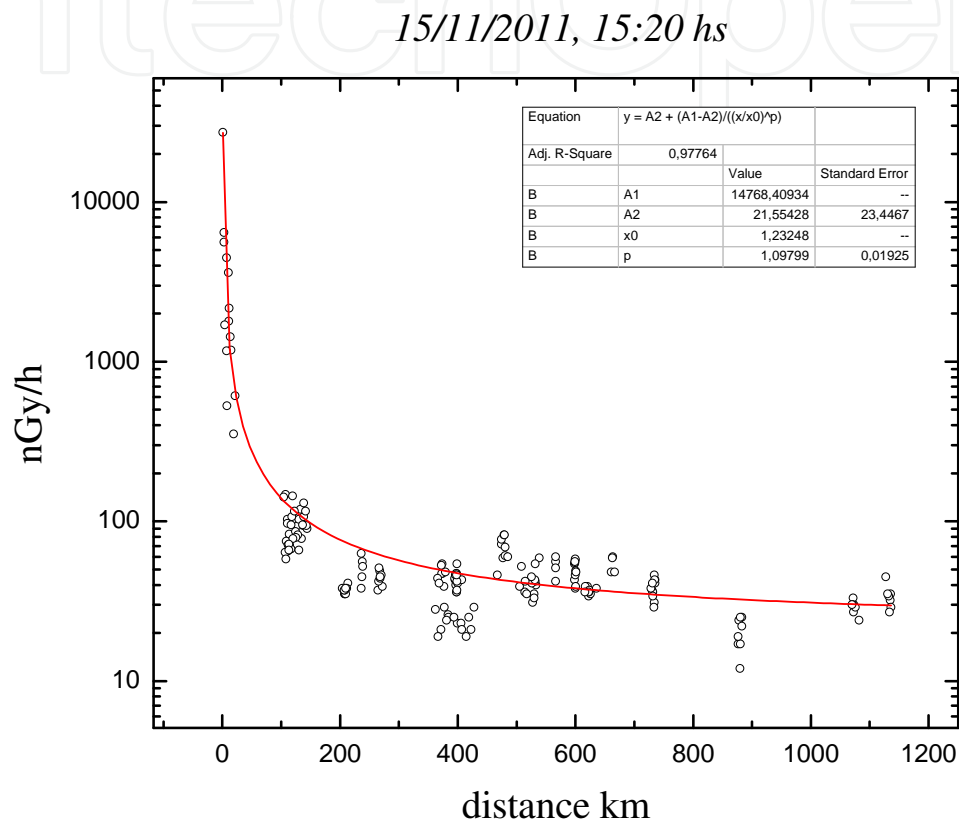


Figure 5. Radiation decrease with distance as November 15, 2011

The Figure 7, shows the radiation decrease with time for the City-Nukata-Naka station, at the Ibaraki prefecture. The decay of the radiation with time is more acute for this station (located at the south of the nuclear power plant). The tail of the distribution can be adjusted with a decreasing exponential with half life 15.6 days (not shown in the graph). The decay of the radiation with time at the nuclear power plant is compatible (although not exactly the same) with the mean life of caesium-137, and strontium-90. The difference between the adjustment and the mean life could disappear with measurements over a larger period of time. Meanwhile, the decrease of radiation at City-Nukata-Naka station has the order of magnitude of the mean life of the iodine-131, and radon-222.

The difference in the decay with time at the two stations can be due to the size of the particulate of each radioactive species, i.e., if the size of the cesium and of the strontium is larger, they could fall closer to the plant. The spectrum of elements in the fallout depends on the

volatility of the isotopes as well, i.e., not all the isotopes produced at the reactor will contaminate a large area. Since the boiling point of each isotope is different, it is expected that the percentage of mass released will be different for each isotope.

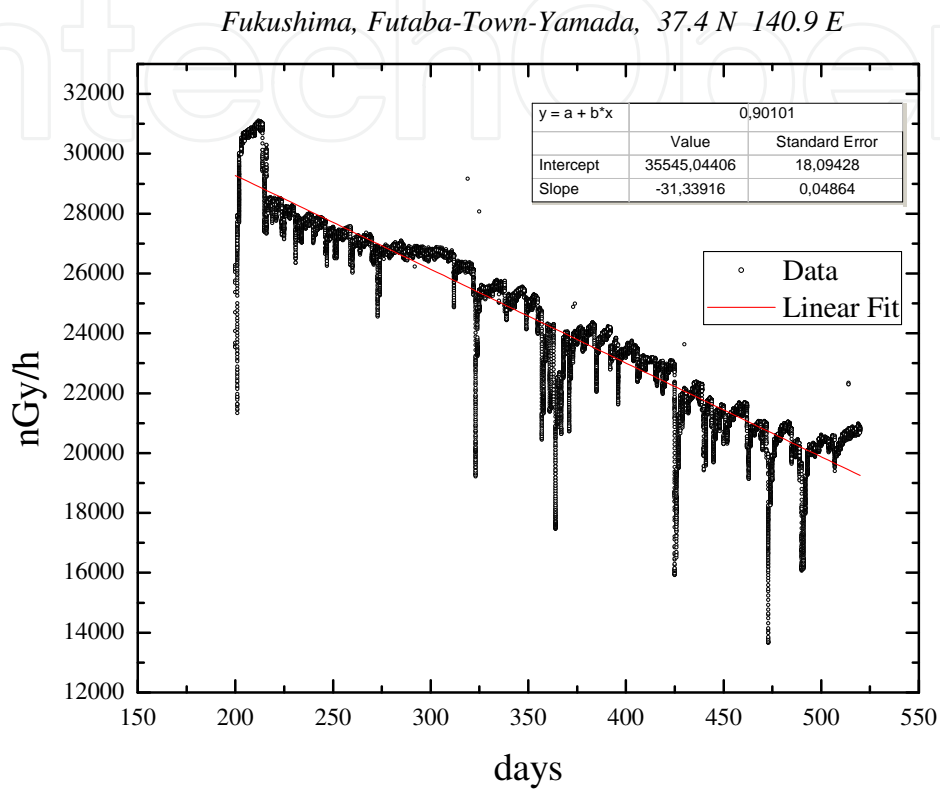


Figure 6. Decrease of the radiation with time at 0.7 km from the nuclear central.

Although there was a stations blackout in the SPEEDi network, TEPCO continued monitoring the radiation at the nuclear power station. These data are not contained within the SPEEDi database analyzed here. The Reference [23] contains data measurements at the nuclear central and presents an artistic representation of the data.

However, is important to note that in the literature is claimed that the TEPCO reports are confusing. Some organizations and news media showed doubts about the published data [30],[31]. As a consequence of this, a global project called Safecast -independently of governments or multinational companies- started to map radiation levels around Japan, using static and moving sensors [30].

On the wake of the disaster, Japan shifted the energetic policy and has plans to drop out nuclear energy by 2030. The decision of the Japan government is accompanied by similar actions of the governments of Germany and Switzerland. On the other hand, Italy has suspended the plans to reinforce the nuclear power in the country [31].

Ibaraki, City-Nukata-Naka, 36.5 N 140.5 E

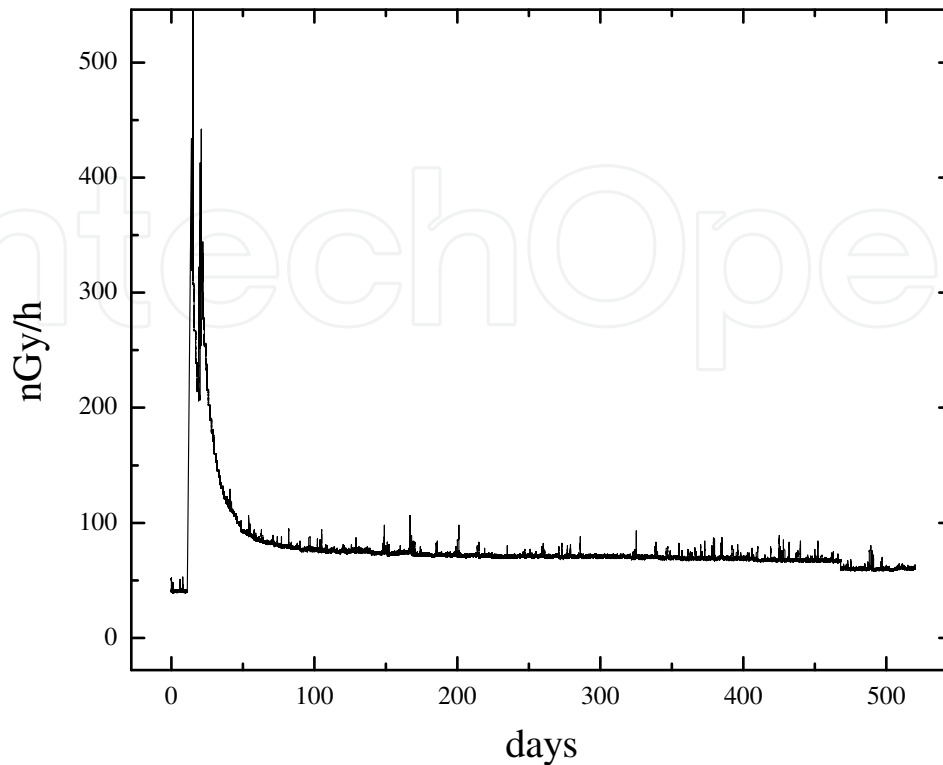


Figure 7. Decrease of the radiation with time at 111 km from the nuclear central.

7. Biological effects of radiation

Biological effects of ionizing radiation depend on dose, dose rate and type of radiation. Dose rates after an accident situation will show large variations in time and position according to meteorological conditions, topography, and whether the area in consideration is urban or rural. Their determination will also be subjected to large uncertainties. Transport characteristics and half life of involved radionuclide will also play a role in determining exposure levels after the accident, as will emergency response and active measures taken regarding the exposed population.

Dose rates after a major accident are dominated in the short time by atmospheric submersion, while most radioactive material is still in suspension. From this source, dose commitment by inhalation is much larger than direct external exposure coming from the radioactive cloud. Given its short half life of 8 days, exposure due to ^{131}I was dominant during the first days after the emissions. Besides, ^{131}I will be absorbed through contaminated food, and will accumulate in the thyroid gland. Its beta particles, with mean energy around 190 keV, have a tissue penetration of 0.6 to 2 mm, and can kill or transform thyroid tissue and affect lung cells if inhaled. Supplying non radioactive iodine in order to saturate thyroid tissue and or

swift evacuation are the recommended procedure. Estimation of dose commitment is usually difficult but a crude number can be derived as follows:

Dose commitment from breathing is around 1.5×10^{-8} Sv/Bq for ^{131}I . Activity concentration was measured at the plant by Tepco and was found to be 1×10^3 Bq/m³ on April 7th, 2011. Dose rate at that particular point would have been 20 $\mu\text{Sv/hr}$, considering a normal breathing rate of about 1.2 m³/hr. However, ^{131}I concentrations must have been orders of magnitude larger shortly after pressure relief events. Moreover, other radionuclides like ^{137}Cs and ^{134}Cs were also suspended in air, though in smaller concentrations. Uncertainties will therefore be large for dose commitment from breath [32].

After contamination plume has passed, main source of radiation is from contaminated material deposited on the ground. ^{137}Cs and ^{134}Cs are the dominant radionuclides that provide the ground shine. ^{137}Cs with a half-life of 30 years is also the main long term contamination source.

In order to make a rough estimate of exposure due to ^{137}Cs , an infinite ground plane uniformly contaminated yielding scatterless photons with a semi isotropic emission pattern is the simplest model that can be considered. A simple geometric calculation for the photon fluence in that model, will show that for a given height above the ground, radiation is dominated by photons travelling horizontally [33]. With a mean free path in air of 280 m for absorption, scatterless photons is quite a good an simple approximation for primary photons. Obtained result shows that the infinite ground plane may not be a particularly good approximation, especially for urban areas. If exposure is dominated by horizontally travelling photons, ground roughness as well as structures above ground level will significantly affect the exposure field. In other words, in order to obtain accurate dose rate conversion factor, i.e., equivalent dose rates for a given ground activity, detailed Monte Carlo calculations would be required. For horizontally travelling isotropic primary photons calculations performed with MC code PENELOPE yield an estimated of 1.3×10^{-12} Sv/(Bq/ m²) 1 m above ground level, which is in agreement with published data for smooth plane surface [33,34].

The Figure 8 shows that the photon fluence from a flat surface at 1 m height is dominated by horizontally travelling photons.

More detailed Monte Carlo calculations show that average dose rate conversion factor yield 2×10^{-12} (Sv/h)/(Bq/ m²) for a fresh contaminated surface. Consequently, accumulated dose for a whole year exposure is around 1.6×10^{-8} Sv/(Bq/ m²). Analog calculation were made for ^{134}Cs , yielding an exposure for the first year of about 3.7×10^{-8} Sv/(Bq/m²)

In order to roughly estimate exposure levels to the areas surrounding Fukushima plant, we can take published values of ^{134}Cs and ^{137}Cs release from the power plant. Different estimates put that quantity in 1×10^{16} Bq for each radionuclide [35]. If we consider the 20 km evacuation zone, and assume half the amount of radioactive material was deposited inside the semicircle with origin in the power plant (with the other half released over the ocean), mean deposition would be 1.6×10^7 Bq/m² for both radionuclides, yielding a 75 mSv/yr average exposure for the first year.

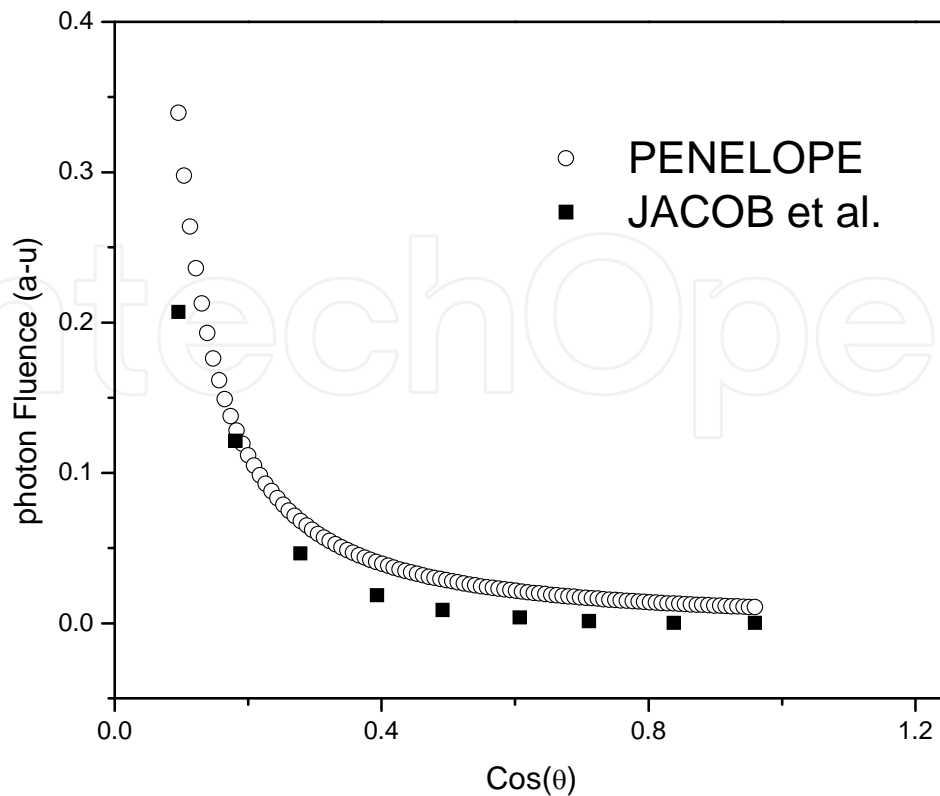


Figure 8. Photon fluence from a flat surface at 1m height

Deterministic radiation effects start at levels above 1000 mSv, but for exposures as low as 100 mSv, statistically significant increases in cancer cases are expected among the exposed population. Assuming that outside the evacuation area, exposure levels will not be higher than the average inside it, which is a conservative assumption, no significant increase in cancer cases should be expected outside the evacuation zone.

Of course, deposition is far from uniform, and a significant amount of Cs-134 and Cs-137 have been carried away by wind. Atmospheric transport models suggest that only 20% of the total release was deposited in Japan land, while 80 % was carried out by wind towards the Pacific Ocean thanks to the prevailing winds during all but one major release events, throughout the emergency [36].

Taking these results into account the average radioactive Cs deposition would fall from 1.7×10^7 Bq/ m² to 6.8×10^6 Bq/ m². and average exposure for the first year inside the 20 km exclusion zone to approximately 15 mSv/yr. Actual deposition maps from flight measurements carried out by DOE show that deposition in Japan soil took place towards the north-west with maximum values for the combined Cs deposition of 1.8×10^7 Bq/ m² close to the plant in the northwest direction. Measurements 20 km away from the plant, in the same direction show numbers around 1×10^6 Bq/ m², which will produce roughly the same exposure as average background natural radiation in Japan (3.8 mSv/yr), but still larger than the 1 mSv/yr exposure limit for the public [37].

8. Conclusion

In this chapter it is given a comprehensive introduction to the Fukushima nuclear accident. A large database of dose measurements taken in time intervals of ten minutes over more than 200 stations was studied using a code specifically designed for it. It is seen that the radiation decays with time following an exponential decay compatible with iodine contamination at large distances. The radiation profile decrease slower than the r^2 law, and seems to become flatter as time goes by. There is a large scatter of radiation, with large variations in distances of the order of a hundred meters, but it seems to become more homogenous with time. Most affected zone is a strip pointing to the northwest of Fukushima. Numeric simulations are performed with the Monte Carlo code PENELOPE to find the equivalence between the published values of the activity and the dose equivalent. It is found that the exclusion zone of 20 km give an exposure of the same order as the background radiation in Japan or less.

Appendix

Chronology of the disaster of Fukushima

	Unit 1	Unit2	Unit 3	Unit 4	Unit 5	Unit 6
March 11, 2011 14:46 JST, earthquake	scrammed	scrammed	scrammed	-	-	-
	loss-of-offsite power lines	loss-of-offsite power lines	loss-of-offsite power lines	loss-of-offsite power lines	loss-of-offsite power lines	loss-of-offsite power lines
	Emergency diesel generators started	Emergency diesel generators started	Emergency diesel generators started	Emergency diesel generators started	Emergency diesel generators started	Emergency diesel generators started
14:50 JST		reactor core isolation system (RCIC) started				
14:52 JST	IC (isolation condenser) automatically actuated					
15:03 JST	IC manually shutdown					
15:05 JST			reactor core isolation system (RCIC) started			

	Unit 1	Unit 2	Unit 3	Unit 4	Unit 5	Unit 6
15:27 JST, 1 st tsunami wave						
15:35 JST, 2 nd tsunami wave	Alternate and direct current power lines were lost	Alternate and direct current power lines were lost	Alternate and direct current power lines were lost	Alternate and direct current power lines were lost	electric power sourced by diesel generator at unit 6	Air cooled electric diesel generator survived
	residual heat removal pumps lost	residual heat removal pumps lost	residual heat removal pumps lost	residual heat removal pumps lost	residual heat removal pumps lost	residual heat removal pumps lost
	High pressure coolant injection (HPCI) inoperable					
18:00 JST	water level reach the top of the fuel, temperature rose					
March 12, 2011 02:44 JST	emergency battery for high pressure core-flooder runs out					
05:30 JST	steam and hydrogen vented into secondary containment					
05:50 JST	Fresh water injection started					
10:58 JST	steam and hydrogen vented into secondary containment					
14:50 JST	fresh water injection halted					
15:36 JST	Hydrogen explosion, secondary containment blown up					
19:00 JST	Sea water injection					
March 13, 2011 02:44 JST	high pressure coolant injection stops					

	Unit 1	Unit2	Unit 3	Unit 4	Unit 5	Unit 6
07:00 JST			water level reaches top of the fuel			
13:00 JST	reactor vented, refilled with water and boric acid. Declared level 4 accident.	stable	reactor vented, refilled with water and boric acid			
March 14, 2011 11:01 JST		water supply damaged by explosion in reactor 3	hydrogen explosion, secondary containment blown up.			
13:15 JST		reactor core isolation cooling system stops				
18:00 JST		water level reaches the top of the fuel				
March 15, 2011 6:00 JST		Explosion in the pressure suppression room.				
11:00 JST		temporary cooling systems damaged by explosion at reactor 3.	second explosion. Radiation rates of 400 mSv/h.	fire breaks out		
March 16, 2011 06:00 JST	Workers withdrawn from the plant					
March 17, 2011 07:00 JST			helicopters drop water on the spent fuel pool. Radiation spike of 3.75 Sv/h. Police and fire trucks sprayed water into the reactor with high pressure hoses.	helicopters drop water on the spent fuel pool		
March 24, 2011	electrical power restored					
August 21, 2011	cold shutdown achieved					

Acknowledgements

We acknowledge Mr. Marian Steinbach for sharing the radiation data sheet and for clarifications about it. CG thanks Mr. Rama Hoetzlein for useful references.

Author details

Cristian R. Ghezzi¹, Walter Cravero^{1,2} and Nestor Sanchez Fornillo¹

1 National University of the South, Department of Physics, Bahía Blanca, Provincia de Buenos Aires, Argentina

2 Institute of Physics of the South, Bahía Blanca, Provincia de Buenos Aires, Argentina

References

- [1] "Nuclear Testing and Nonproliferation", <http://www.iris.iris.edu/HQ/Bluebook/contents.html>
- [2] "Fukushima faced 14-metre tsunami", World Nuclear News, http://www.world-nuclear-news.org/RS_Fukushima_faced_14-metre_tsunami_2303113.html
- [3] TEPCO press release 3, 2011, <http://www.tepco.co.jp/en/press/corp-com/release/11031103-e.html>
- [4] Japan earthquake update (2210 CET), IAEA press release, 2011, <http://www.iaea.org/press/?p=1133>
- [5] United States Nuclear Regulatory Commission Technical Training Center, The Boiling Water Reactor Systems: Reactor Concepts Manual, 2009.
- [6] GENERAL ELECTRIC, Boiling Water Reactor GE-BWR4 Technology, Technology Manual, chapter 6: BWR Differences, Editor: United States Nuclear Regulatory Commission Technical Training Center, 2009.
- [7] "Insights from review and analysis of the Fukushima Dai-ichi accident", Hirano M., Yonemoto T., Ishigaki M., Watanabe N., Maruyama Y., Sibamoto Y., Watanabe T., and Moriyama K., 2012, Journal of Nuclear Science and Technology, 49, 1.
- [8] Wikipedia, "Fukushima Daiichi Nuclear Disaster", http://en.wikipedia.org/wiki/Fukushima_Daiichi_nuclear_disaster#cite_note-tepco11b-75
- [9] Gundersen A., <http://fairewinds.org/content/gundersen-postulates-unit-3-explosion-may-have-been-prompt-criticality-fuel-pool>

- [10] Cottingham W. N., & Greenwood D. A., "An introduction to nuclear physics", Cambridge University Press, 1986.
- [11] "How Much Spent Nuclear Fuel Does the Fukushima Daiichi Facility Hold?" Scientific American, March 17 2011, <http://www.scientificamerican.com/article.cfm?id=nuclear-fuel-fukushima>
- [12] Murray R. L., "Nuclear energy: An Introduction to the Concepts, Systems, and Applications of the Nuclear Processes", Butterworth-Heinemann, 2001.
- [13] Lewis, E. E., "Fundamentals of Nuclear Reactors Physics", Academic Press, 2008.
- [14] United States Nuclear Regulatory Commission, <http://www.nrc.gov/reading-rm/doc-collections/fact-sheets/>
- [15] Wikipedia, "MOX fuel", http://en.wikipedia.org/wiki/MOX_fuel
- [16] Fukushima Nuclear Accident Analysis Report, Tokyo Electric Power Company (TEPCO), June 20, 2012.
- [17] Fukushima Daiichi Status Report, International Atomic Energy Agency, April 27, 2012.
- [18] Wikipedia, "Fukushima Daiichi Nuclear Power Plant", http://en.wikipedia.org/wiki/Fukushima_Daiichi_Nuclear_Power_Plant#cite_note-pu-7
- [19] United States Nuclear Regulatory Commission, Technical Training Center, Chattanooga, TN, "Boiling Water Reactor Systems: Reactor Concepts Manual", <http://www.nrc.gov/reactors/power.html>.
- [20] Japan Radiation Map, 2012, <http://jciv.iidj.net/map/>.
- [21] Steinbach, M., "A Crowd Sourced Japan Radiation Spreadsheet", 2012, <http://www.sendung.de/japan-radiation-open-data/>
- [22] GebWeb, <http://gebweb.net/blogpost/2011/03/17/japan-radiation-map/>
- [23] Hoetzlein, R., Leonardo, "Visual Communication in Times of Crisis: The Fukushima Nuclear Accident", 24, 2, 113, 2012; <http://www.rchoetzlein.com>.
- [24] "Radiation Measuring Station Locations", SPEEDi (System for Prediction of Environmental Emergency Dose Information), <http://goo.gl/iDo0N>
- [25] "Occupational Dose Limits", United States Nuclear Regulatory Commission, <http://www.nrc.gov/reading-rm/doc-collections/cfr/part020/part020-1201.html>
- [26] Villarreal, E., <http://public.tableausoftware.com/views/JapanRadiationLevels/JapanRadiationLevelsDashboard>
- [27] "Fukushima radioactive fallout nears Chernobyl levels", New Scientist, March 24, 2011.

- [28] "Japanese nuclear firm admits error on radiation reading", The Guardian, 27 March 2011, <http://www.guardian.co.uk/world/2011/mar/27/japan-nuclear-error-radiation-reading>
- [29] "Fukushima radiation higher than first estimated", Reuter, Kevin Krolicki, May 24, 2012.
- [30] Safecast, 2012, blog.safecast.org.
- [31] "Japan targets phasing out nuclear power in 2030s", The Mainichi, September 15, 2012.
- [32] Journal of Environmental Radioactivity, 109, 103, 2012.
- [33] Saito and P. Jacob, Radiation Protection Dosimetry, 58, 29, 1995.
- [34] F. Salvat, J.M. Fernández-Varea and J. Sempau, "PENELoPE-2008: A Code System for Monte Carlo Simulation of Electron and Photon Transport", OECD Nuclear Energy Agency, Issy-les-Moulineaux, France, 2008.
- [35] Chino et al., J. Nucl. Sci. Tec., 48, 1129, 2011
- [36] A. Stohl et al, J. Chem. Phys., 12, 2313, 2012
- [37] U.S. Department of Energy: <http://energy.gov/articles/us-department-energy-releases-radiation-monitoring-data-fukushima-area>

IntechOpen